JOURNAL OF GEOPHYSICAL RESEARCH, VOL. 104, NO B12, PAGES 29,419-29438, DECEMBER 10, 1999

A method for evaluating basement exhumation histories from closure age distributions of detrital minerals

Oscar M. Lovera and Marty Grove

Department of Earth and Space Sciences and Institute of Geophysics and Planetary Physics, University of California, Los Angeles

David L. Kimbrough and Patrick L. Abbott

Department of Geological Sciences, San Diego State University San Diego, CA 92182-1020

Abstract. We have developed a two-dimensional, thermo-kinetic model that predicts the closure age distributions of detrital minerals from pervasively intruded and differentially exhumed basement. Using this model, we outline a method to determine the denudation history of orogenic regions on the basis of closure age distributions in synorogenic to postorogenic forearc strata. At relatively high mean denudation rates of 0.5 km m.y.$^{-1}$ sustained over millions of years, magmatic heating events have minimal influence upon the age distributions of detrital minerals such as K-feldspar that are moderately retentive of radiogenic Ar. At lower rates however, the effects of batholith emplacement may be substantial. We have applied the approach to detrital K-feldspars from forearc strata derived from the deeply denuded Peninsular Ranges batholith (PRB). Agreement of the denudation history deduced from the detrital K-feldspar data with thermochronologic constraints from exposed PRB basement lead us to conclude that exhumation histories of magmatic arcs should be decipherable solely from closure age distributions of detrital minerals whose depositional age is known.

1. Introduction

Clastic sedimentary sequences shed from orogenic belts provide a fertile, and arguably unique, record of crustal exhumation. It has long been recognized that isotopic age analysis of chemically resistant detrital minerals such as zircon and muscovite presents a promising tool for provenance and paleogeography studies [e.g., *Abdel-Monen and Kulp*, 1968; *Ledent et al.*, 1964]. Refinement of U-Pb, $^{40}Ar/^{39}Ar$, and fission track methods for rapid and comparatively precise age analysis of single crystals over the past several decades have greatly benefited detrital-mineral dating [e.g., *Gaudette et al*., 1981; *Fronde et al*., 1983; *Hurford et al*., 1984; *Kelley and Bluck*, 1989]. While use of the technique is now routine in provenance studies [e.g., *Garver and Brandon*, 1994a*; Gehrels et al.*, 1995; *Dallmeyer et al.*, 1997; *Ireland et al*., 1998; *Hutson et al*., 1998], its potential for recovery of basement exhumation histories has not been widely exploited [*Copeland and Harrison*, 1990; *Renne et al.*, 1990; *Corrigan and Crowley*, 1992; *Harrison et al*., 1993; *Garver and Brandon*, 1994a,b; *Clift et al.*, 1996].

Denudation studies based upon isotopic dating methods fundamentally assume that retention of radioactive decay products within minerals is governed by volume diffusion [*McDougall and Harrison*, 1999]. Measured ages are interpreted in terms of bulk isotopic closure which can be equated with depth in the crust (i.e., closure depth) provided that the geotherm is reasonably estimated [*Dodson*, 1973]. Hence a spectrum of closure ages yielded by detrital grains from a dated sedimentary horizon contains information on the distribution of crustal depths exposed in the basement terrane at the corresponding time of erosion. Meaningful interpretation of these results in terms of basement exhumation rates requires complete representation of the basement erosion surface and effectively instantaneous sediment transport. Assessments are further complicated by the necessity of independently determining sediment provenance and/or evaluating possible diffusive loss of radioactive decay products during burial.

The approach generally taken in denudation studies based upon detrital mineral dating has been to estimate exhumation rates from the ratio of closure depth and the time lag between isotopic closure and time of erosion. This time interval has been defined differently depending upon the focus of researchers. Consideration of the youngest closure ages in a detrital suite yields maximum denudation rates [e.g., *Copeland and Harrison*, 1990] while use of a central age maxima in the distribution returns a mean denudation rate [e.g., *Garver & Brandon*, 1994b]. Closure depth is also difficult to establish since it requires knowledge of the basement thermal structure at the time of closure and the diffusion properties or annealing kinetics of the thermochronometer. Depths have been estimated either from empirical data [e.g., *Renne et al.*, 1990] or calculated from experimental diffusion parameters or annealing kinetics [*Clift et al.*, 1996]. Regardless, calculations of exhumation history

Paper number 1999JB00082
0148-0227/99/1999JB900082$09.00

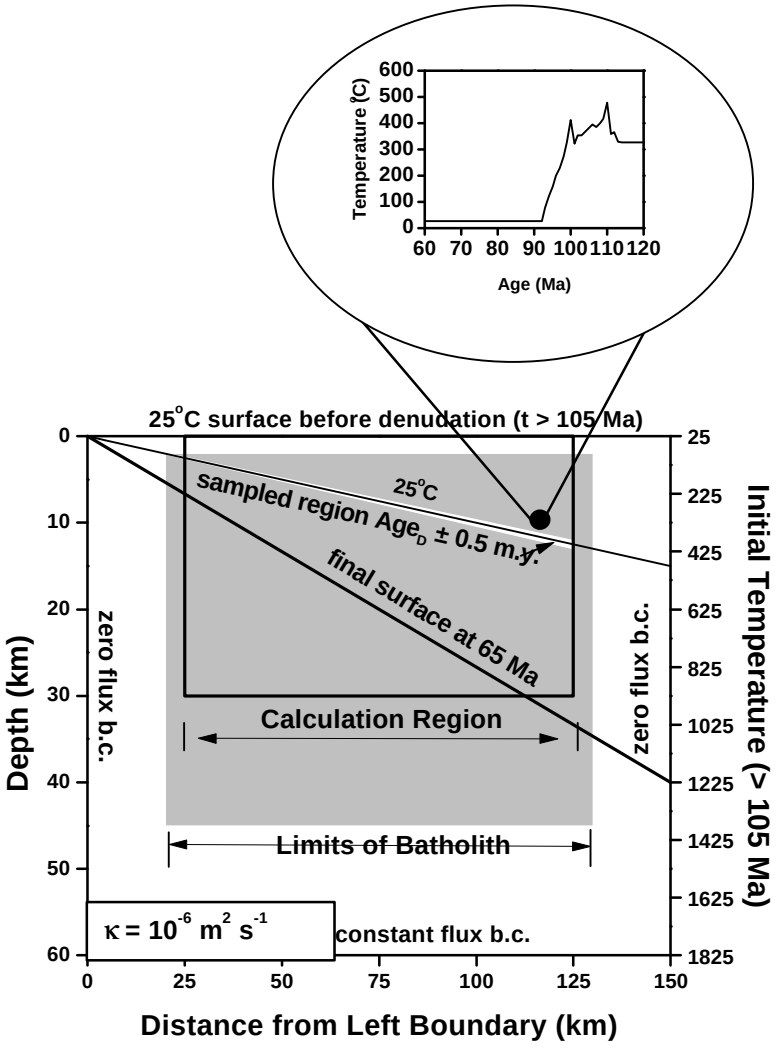

Figure 1: Schematic of numerical model illustrating scaling and boundary conditions. The shaded portion of the grid indicates where closure ages are calculated. Samples assigned to a given depositional age (Age_D) are from ±0.5 m.y. region. The bold line is the final (65 Ma) surface.

have invariably assumed a steady state thermal structure. This can be a poor assumption, particularly in batholithic terranes formed by pervasive pluton emplacement [*Hanson and Barton*, 1989].

In this paper we introduce an approach for predicting closure age distributions from detrital minerals that originate from batholithic source regions. While we focus upon differentially exhumed arc crust, the method provides the basis for studying other tectonic settings amenable to representation by two-dimensional models. The approach differs significantly from that of *Stock and Montgomery* [1996] who assume horizontal isothermal distributions and complete isotopic closure prior to denudation to estimate paleorelief. We numerically simulate spatially variable pluton emplacement and denudation with thermo-kinetic models and use the resulting temperature-time histories for individual grid points to calculate bulk closure ages over the entire region. Erosion is simulated by sweeping the upper boundary through the grid and randomly sampling between successive erosion surfaces. Protocols for comparing measured and synthetic closure age distributions employ the Kolmogorov-Smirnov statistic and provide the basis for forward modeling of denudation rates in the source region. Provided that denudation outlasts intrusion and sufficient erosion has occurred, we find that the results are highly sensitive to exhumation rate and indifferent to intrusion history and/or the time of initial denudation.

To more fully illustrate our approach, we have modeled detrital K-feldspar closure age distributions from Cretaceous forearc basin strata derived from the Peninsular Ranges batholith in southern and Baja California. K-feldspar, a common mineral in first-cycle continental margin sediments offers distinct advantages over other detrital thermochronometers for investigating basement denudation. General agreement of the exhumation history deduced from detrital K-feldspar results with independent thermochronology from the basement lead us to conclude that exhumation histories of magmatic arcs, or any other highly strongly denuded orogen, should be decipherable solely from closure age distributions from detrital minerals.

2. Model Description

Intrusion and denudation operate individually or in concert in our model. We calculate thermal histories for arc detritus using a 2-D, Crank-Nicholson finite-difference algorithm to solve the diffusion equation (*Press, et al*. 1986, p. 638). Boundary conditions include zero lateral-flux, constant surface temperature (25°C), and a constant basal heat flux (Figure 1). Heat conduction is described in a simple manner by maintaining thermal diffusivity at a constant value (10^{-6} m^2/sec), neglecting radioactive internal heating, and fixing the basal heat flux at an appropriate value to maintain a 30°C/km thermal gradient in the absence of intrusion or denudation.

2.1. Thermal Effects of Batholith Emplacement

We simulate batholith formation in a manner that permits description of complex intrusion geometries [see *Hanson and Barton*, 1989]. Random distributions of circular plutons are instantaneously emplaced at successive times (Plate 1). Thermal effects of intrusion are simulated by setting the temperature of grid points within pluton boundaries to magmatic values at the time step corresponding to emplacement. The initial temperature assigned to a given pluton is a randomly selected value between 850-1000°C. Spatial characteristics of the pluton distributions are allowed to vary between imposed limits. Centers of plutons are restricted to positions further than 20 km from lateral boundaries and at least 15 km above the base of the grid while tops of plutons are required to be at least 2 km below the surface at the time of emplacement (Figure 1). Superposition of intrusions is allowed within a given time frame (Plate 1). Partial obliteration of the older intrusions occurs in successive intervals (Plate 2). Host rock deformation and/or assimilation during intrusion is not considered.

To illustrate the effect of intrusion history upon closure age distributions, we have investigated two emplacement sequences (Plate 2). The first (Plate 2a) involves uniform random intrusion while the second (Plate 2b) simulates a shift in the locus of intrusion. The cumulative intrusion density produced in either sequence is comparable to that observed in many Cordilleran batholiths [ca. 15% host rocks remain; *Barton et al*., 1988].

2.2. Denudation, Erosion, and Deposition

Denudation is simulated by redefining the position of the earth's surface in the model through the grid in successive time steps. This is accomplished by setting the temperature of all grid points situated at or above the defined surface to a constant value (25°C). The time (Age_D) at which material at a given grid point is "eroded" is defined as that corresponding to passage of the 25°C surface beneath it (Figure 1). We consider all material bounded by surfaces ± 0.5 m.y. from Age_D to be deposited at Age_D. This ensures that the amount of sediment eroded at a given lateral position is proportional to the denudation rate. While the definition of the 25°C surface can be quite general, we opted to simulate only linear denudation (i.e., tilting of a planar surface) in the present paper. In each simulation, the axis of rotation is fixed at the upper left corner of the grid and the movement of the surface towards grid points is clockwise so that samples in the right-hand portion of the grid experience the greatest denudation. Although a constant rate of rotation is applied in early models, we later introduce a time dependence for this parameter to demonstrate the ability of the model to fit measured data. In each simulation we initiate denudation at 105 Ma. Note that because the time of initial denudation is arbitrary fixed, the magnitude of denudation required to fit measured results is necessarily a relative quantity. However, as will be shown subsequently, our estimates of denudation rates do not depend strongly upon when we initiate erosion provided that sufficient exhumation has occurred to expose thermochronometers that were deep enough to be partially open to Ar loss.

2.3. Calculation of Closure Age Distributions

Each run of the model calculates temperature-time (T-t) histories for all points within the upper 30 km of the grid. From this set of T-t paths, bulk closure ages are computed using a single domain diffusion model and experimentally determined Arrhenius parameters for K-feldspar (activation energy or E = 46.5 kcal/mol; frequency factor or log D_o/r_o^2 = 5.0 s^{-1}; *Lovera et al*., 1997). Sampling of detrital closure ages is performed using random deviates with a uniform probability distribution and the transformation method described by *Press et. al* [1986, p. 200-203]. The probability that a closure age corresponding to a given horizontal position along the erosion surface will be sampled is proportional to the denudation rate at that location at time Age_D. Since sample points do not generally coincide with grid points, closure ages are computed by interpolation. To avoid possible complications arising at lateral boundaries of the model, we only sampled horizontal positions between 25-125 km (Figure 1).

2.4. Comparison of Model Results with Measured Age Distributions

A crucial element for our method is an appropriate protocol for evaluating the similarity of measured and model distributions. We have applied the Kolmogorov-Smirnov (K-S) statistic [*Press et al*., 1986, p.475], a generally accepted test to compare populations. Because the parameter produced by the K-S statistic (D) is defined as the maximum value of the absolute difference between two cumulative distribution functions, it is most sensitive to the overall character of cumulative distributions and relatively insensitive to outlying data.

A major benefit of the K-S statistic is that the numerical significance of D, defined as *PROB*, can be assessed for the null hypothesis (i.e., data sets from the same distribution). Values of *PROB* near unity indicate that two distributions are similar while values approaching zero imply significantly different distributions. To evaluate the sensitivity of *PROB* in our application, we sampled detrital closure ages corresponding to a single Age_D value in different ways and applied the K-S test. This exercise entailed systematically comparing 100 cumulative distribution functions (each defined by 32 randomly selected detrital closure ages) with a distribution function represented by a larger sampling based upon 1000 detrital closure ages from the same result. We found that the resulting log(*PROB*) values varied from -1.6 to 0 with a mean value of ~-0.4 and conclude that the sensitivity of the K-S test in terms of log(*PROB)* units is ~1 for

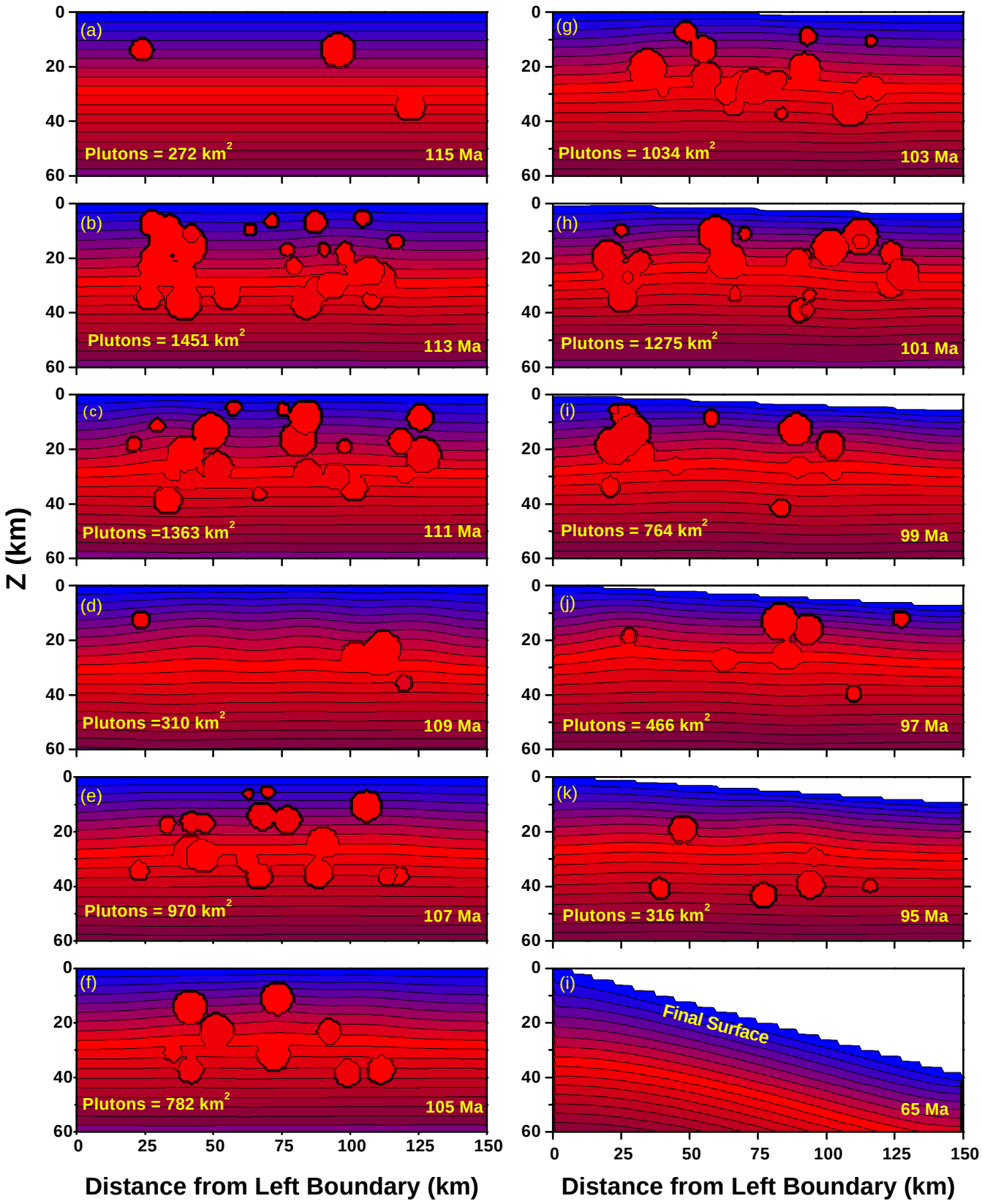

Plate 1: Development of batholith thermal structure in Model II. Isotherms begin at 25°C and are spaced at 100°C. The net area intruded in lower left-hand panel corners. The red tinged regions represent conditions where K-feldspar retains no radiogenic Ar. (a)-(f) Distribution of isotherms in batholith prior to the onset of denudation (115-105 Ma); (h-k) Thermal structure for times characterized by simultaneous intrusion and denudation (105-95 Ma). (l) Final thermal structure at 65 Ma.

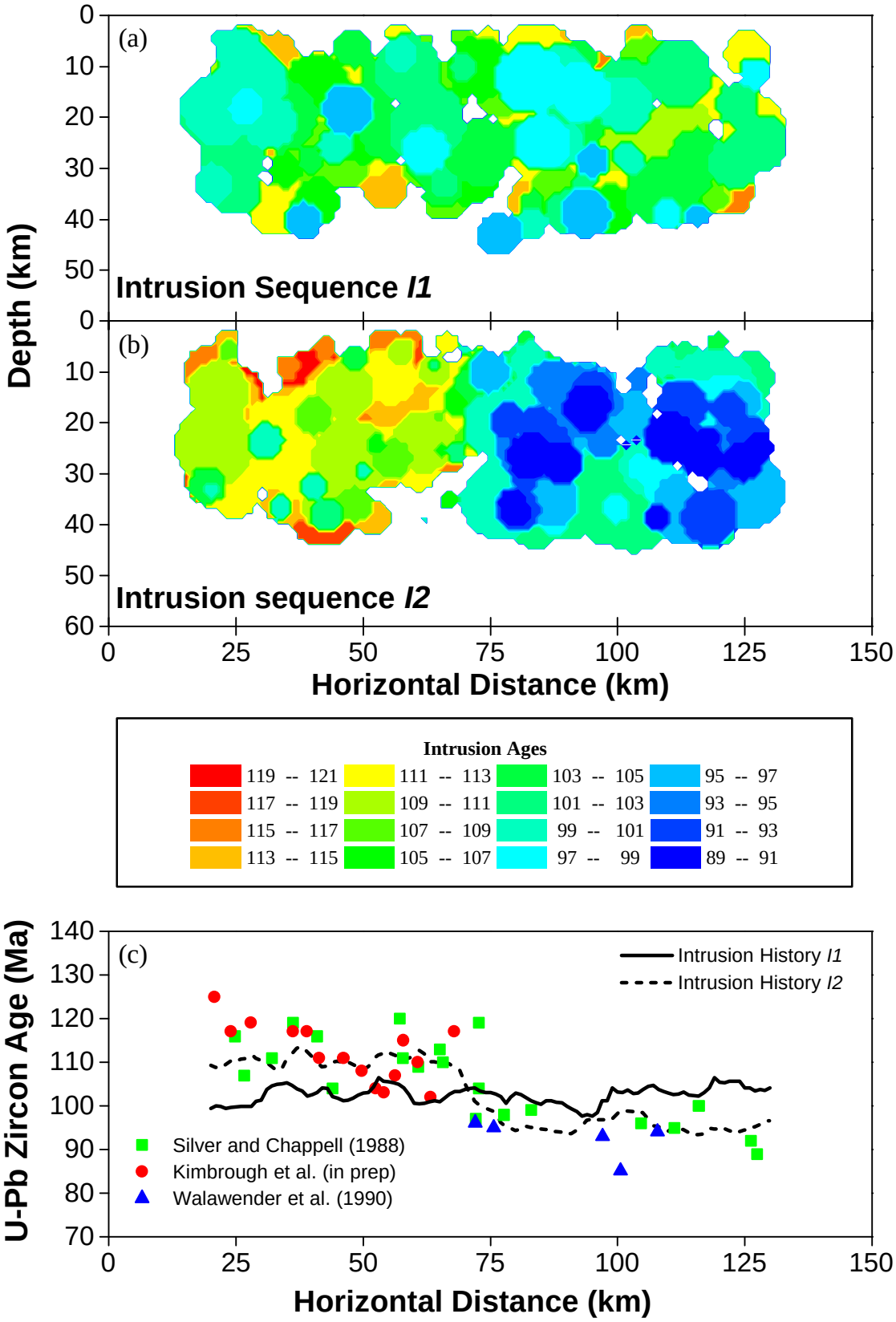

Plate 2: Contours of emplacement age for final pluton distributions in (a) *I1*and (b) *I2*. (c) Mean intrusion age of plutonic rocks versus horizontal distance. Values for *I1* and *I2* are represented by solid and dashed lines, respectively. Zircon U-Pb ages [*Silver and Chapple*, 1988; *Walawender et al.*, 1990; D. L. *Kimbrough*, unpublished data, 1998] from the rectangular region in Figure 3

cumulative distribution functions calculated from small samples.

Our approach for comparing measured detrital age distributions with those produced by the model is summarized in Figure 2. In this example, we compare measured closure ages with those produced by a representative run of the model. To determine the model age distribution that best matches the measured distribution, we obtain synthetic distributions corresponding to different values of Age_D and apply the K-S test to determine which of the distributions represents the maximum value of *PROB* ($PROB_{max}$; Figure 2a). We refer to the Age_D value corresponding to $PROB_{max}$ as Age_D^{max} and define the difference between the stratigraphic age (Table 1) and Age_D^{max} as *Dt*. Model results for Age_D values within ±4 m.y. of Age_D^{max} are compared with the measured detrital age distribution in Figures 2 b-f. The model distribution corresponding to Age_D^{max} is shown in Figure 2d. Age_D distributions ±2 m.y. from Age_D^{max} yield log(*PROB*) values of ~-3 and can just be resolved from the measured distribution (Figures 2c and 2e). Alternatively, Age_D distributions ±4 m.y. from Age_D^{max} yield much lower *PROB* values (< -7) and are easily distinguished from the measured data (Figures 2b and 2f). The asymmetry in *PROB* about Age_D^{max} results from the definition of the K-S statistic and the nature of the distribution functions. However, the rate at which *PROB* drops off on either side of Age_D^{max} is strongly influenced by the denudation rate.

3. A Case Study: The Northern Peninsular Ranges Batholith

We now illustrate our approach to determining the exhumation history of arc crust from closure age distributions by analyzing detrital K-feldspars from Late Cretaceous forearc basin strata shed from the PRB of southern California (Figure 3). Because the sampled strata rest directly upon the western margin of the PRB, contain a clast assemblage derived from the PRB, and exhibit structures indicating west-directed transport [*Girty*, 1986; *Kimbrough et al*., 1997] their genetic relationship to the batholith is assured. A combination of factors identifies the northern PRB as an appropriate setting to develop and test the methods presented in this paper. Most of the 800 km-long PRB was intruded 120-90 Ma [*Silver and Chappell*, 1988]. In its northern extent, the density of intrusion was sufficiently high (85-90%) [*Barton et al.,* 1988] to reset prebatholithic thermochronometers from all but the shallowest crustal levels. Correlation of K-Ar mineral age with depth of erosion points to denudation as the primary control for causing Ar closure in biotite and K-feldspar [*Krumenacher et al.*, 1975; *Grove*, 1993]. Erosion depth increases from <0-5 km in the west to 15-20 km in the east [*Ague and Brimhall*, 1988; *Todd et al*., 1988]. Eastward increase in paleodepth appears to have involved westward tilting of the batholith [*Butler et al*., 1991; *George*, 1993; *Ortega Rivera* et al., 1997; *Dickinson and Butler*, 1998]. However, W-directed thrusting [*Engle and Schultejann*, 1984; *Todd et al*., 1988; *Goodwin and Renne* 1991; *Grove*, 1993], and E-directed extensional faulting [*Erskine and Wenk*, 1985; *Gastil et al*., 1992; *George and Dokka*, 1994] also appear to have played a role in establishing the present depth distribution. Unroofing of all but the easternmost PRB was largely complete by the end of the Cretaceous. Tertiary stability of the PRB is indicated by > 60 Ma apatite fission track ages [*Dokka*, 1984; *George and Dokka*, 1994], preservation of Paleocene paleosols, Eocene erosional surfaces, and fluvial systems that extended from

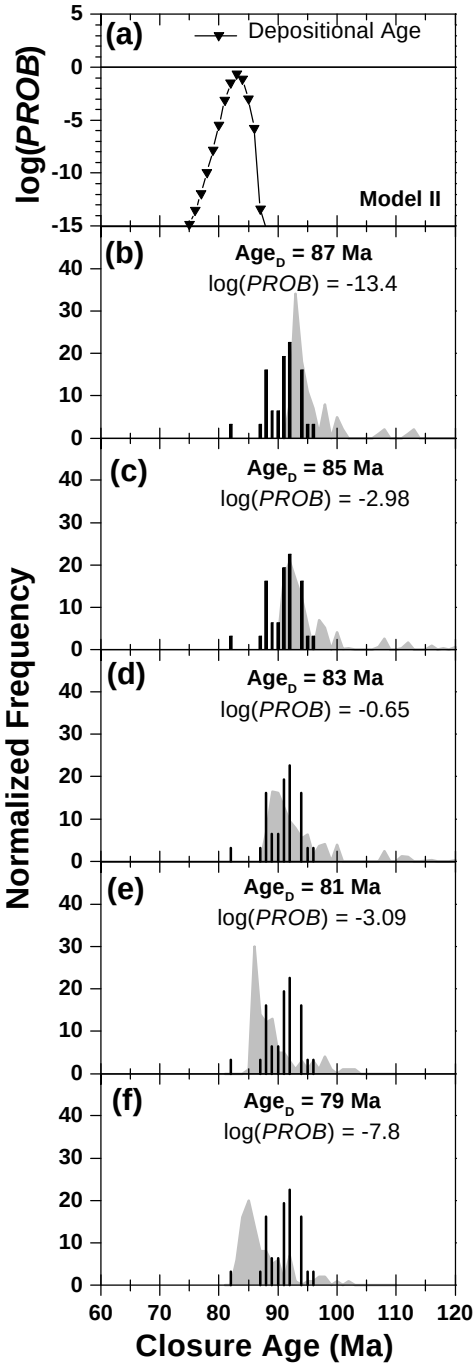

Figure 2: (a) Kolmogorov-Smirnov (K-S) statistical comparison of model and measured closure age distributions. The quantity *PROB* represents the significance level of K-S statistic. Depositional age and uncertainty for the Mustang Spring sample indicated above. (b)-(f) Comparison of model (shaded) and measured results (black) for Age_D = 87, 85, 83, 81, and 79 Ma. All data are normalized to 100.

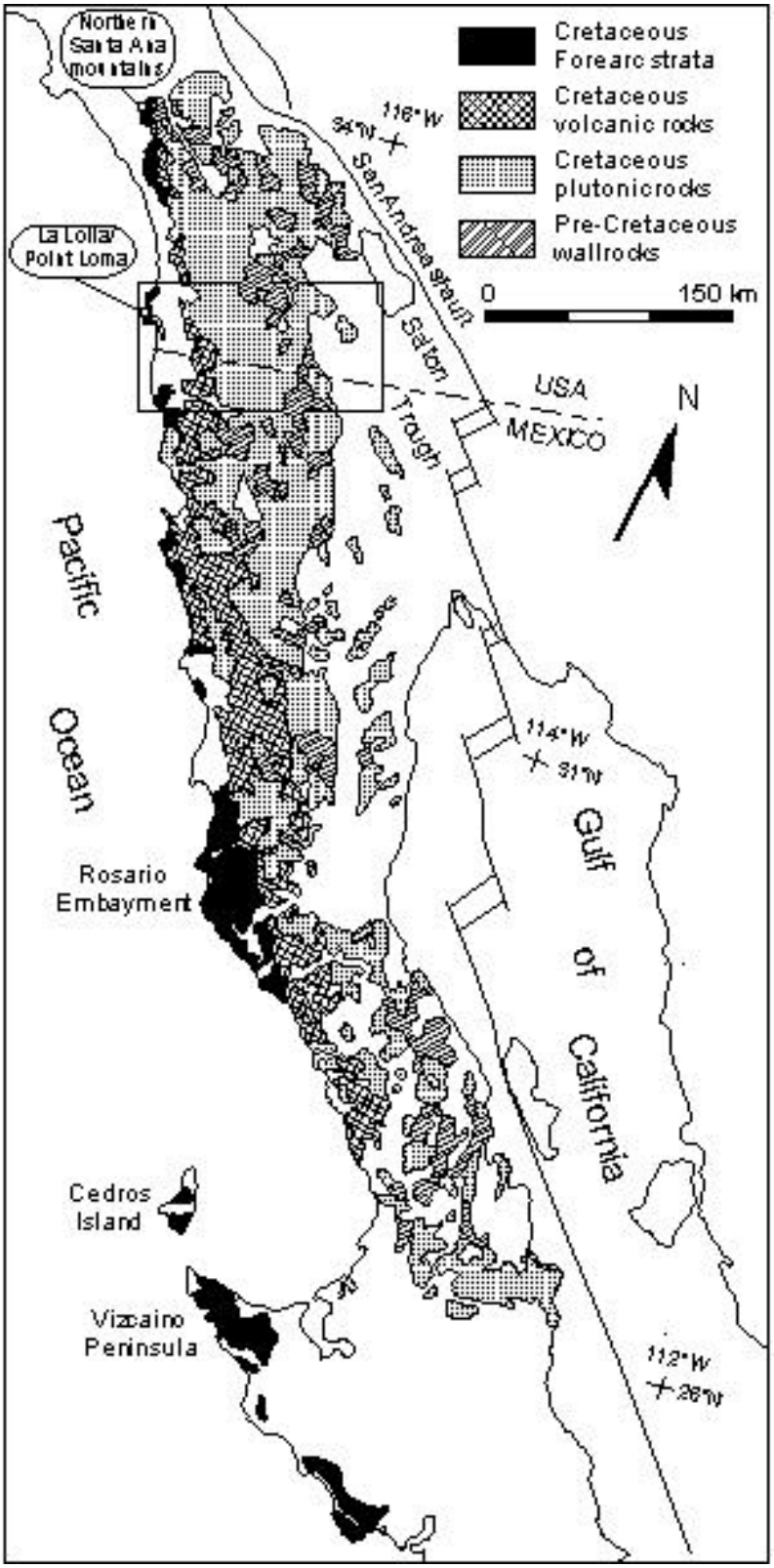

Figure 3: Generalized geologic map of the Peninsular Ranges batholith (PRB). Sampled locations in the northern Santa Ana mountains(NSA) and La Jolla/Point Loma area are indicated. Rectangle (150 x 80 km) represents the region from which thermochronologic data shown in subsequent figures are obtained

Table 1 Depositional Age Constraints

Sample Name	Stratigraphic Unit	Sample Location Latitude/ Longitude	Magnetostratigraphy (Chron)[1]	Time Scale Position	Estimated Age (Ma)
Tourmaline Beach	Cabrillo Formation	N32°48'26" W117°15'49"	32N	upper Campanian	73^{+4}_{-2}
Bird Rock	Upper Point Loma Fm.	N32°48'50" W117°16'22"	32R2	upper Campanian	74^{+3}_{-1}
La Jolla Bay	Lower Point Loma Fm.	N32°51'07" W117°15'38"	33N	mid Campanian	76^{+3}_{-1}
Williams	Williams Formation	N33°45'26" W117°39'21"	C33N/C32R2	mid Campanian	75^{+1}_{-3}
Mustang Springs	Mustang Spring Member	N33°45'32" W117°38'33"	C33R	lower Campanian	80^{+3}_{-4}
Baker Canyon	Baker Canyon Member	N33°44'51" W117°38'29"	C34N	Turonian	90^{+1}_{-1}
Trabuco	Trabuco Formation	N33°44'51" W117°38'17"	C34N	Cenomanian-Turonian (?)	92^{+10}_{-2}

[1]Based on *Gradstein et al.* [1994]

mainland Mexico across the PRB to the coast [*Minch*, 1979; *Abbott and Smith*, 1989].

We have analyzed detrital K-feldspars from sandstones sampled from the Point Loma and Cabrillo Formations west of San Diego (Figure 4a) and from the Trabuco, Baker Canyon, Mustang Spring, and Williams Formations within the northern Santa Ana Mountains (Figure 4b; see Table 1 for localities). Details of the $^{40}Ar/^{39}Ar$ laser fusion analysis appear in Appendix A. Trabuco Formation sandstone is immature biotite litharenite with subequal amounts of metamorphic and sedimentary lithics and minor volcanic lithics. All stratigraphically higher sandstones are biotite feldspathic arenites [cf. *Girty*, 1986]. Depositional age constraints for each of the samples are given in Table 1 (for details see Appendix B). As indicated, uncertainties of ~2-3 m.y. apply to most estimates.

4. Results

4.1. Closure Age Distributions From the PRB Forearc Sediments

Single-grain, total fusion $^{40}Ar/^{39}Ar$ ages determined for 30-70 individual K-feldspar grains extracted from each of the seven samples are displayed in Figure 4c-i. Tabulated $^{40}Ar/^{39}Ar$ data are available from http://oro.ess.ucla.edu.

4.1.1. Provenance. The narrow age range (~75 to 105 m.y.) yielded by all of the K-feldspars closely overlaps that observed for the PRB basement. The paucity of closure ages older than 100 Ma in these samples indicates that shallow-level intrusions of the western PRB which yield K-Ar biotite and U-Pb zircon ages of ~105-120 Ma [*Krummenacher et al.*, 1975; *Silver and Chappell*, 1988] contributed insignificant quantities of sand to these strata. Likewise, sources of sand exogenous to the PRB appear nil or absent. Results from the Trabuco Formation sample (Figure 4I) indicate its depositional age must be <95 Ma; this provides a much tighter constraint on the stratigraphic age of the Trabuco than has been heretofore available. Closure ages that are up to 4 m.y. younger than the estimated depositional age of the overlying Baker Canyon unit (Figure 4h) are clearly problematic and likely indicate either overestimation of its depositional age, ^{40}Ar loss during diagenesis, and/or unrecognized analytical difficulties.

4.1.2. Basement Exhumation Rates. As outlined in the introduction, the commonly employed, first-order approach for estimating exhumation rates from detrital data involves dividing the closure depth by the time lag between the closure age and the time of erosion/deposition. For the sake of illustration, we define the closure age as the mean value of the age distribution. The time lag for the syn-orogenic samples (Trabuco and Baker Canyon; Figure 4h-i) is roughly 5 m.y. while that indicated for post-orogenic samples is somewhat larger (ca. 12 m.y.) though more difficult to characterize. If we arbitrarily assign a closure depth for K-feldspar of 5 km, these lag times indicate mean denudation rates of 1 km/m.y. during the Cenomanian-Turonian and ca. 0.4 km/m.y. after final intrusion within the batholith. Below we investigate how these estimates are affected by pervasive magmatic reheating within the source region.

4.2. Numerical Simulation of Closure Age Distributions from Magmatic Arcs

In order to illustrate how intrusion and denudation interact to affect our results, we ran the program for different combinations of intrusion (Plate 2) and denudation (Table 2). The specific permutations employed in the first six models are outlined in Table 3. We examine results from models I (Figure 5) and II (Figure 6) in detail. Predicted detrital age distributions shown in Figure 7 illustrate how varying denudation rate and intrusion history influences the outcome (see also Table 3). We conclude the section by examining how variation in the time of initial exhumation and the diffusion parameters affect the results.

4.2.1. Denudation without Intrusion. Important effects observed in all our simulations are clearly demonstrated in Model I. The distribution of K-feldspar closure ages

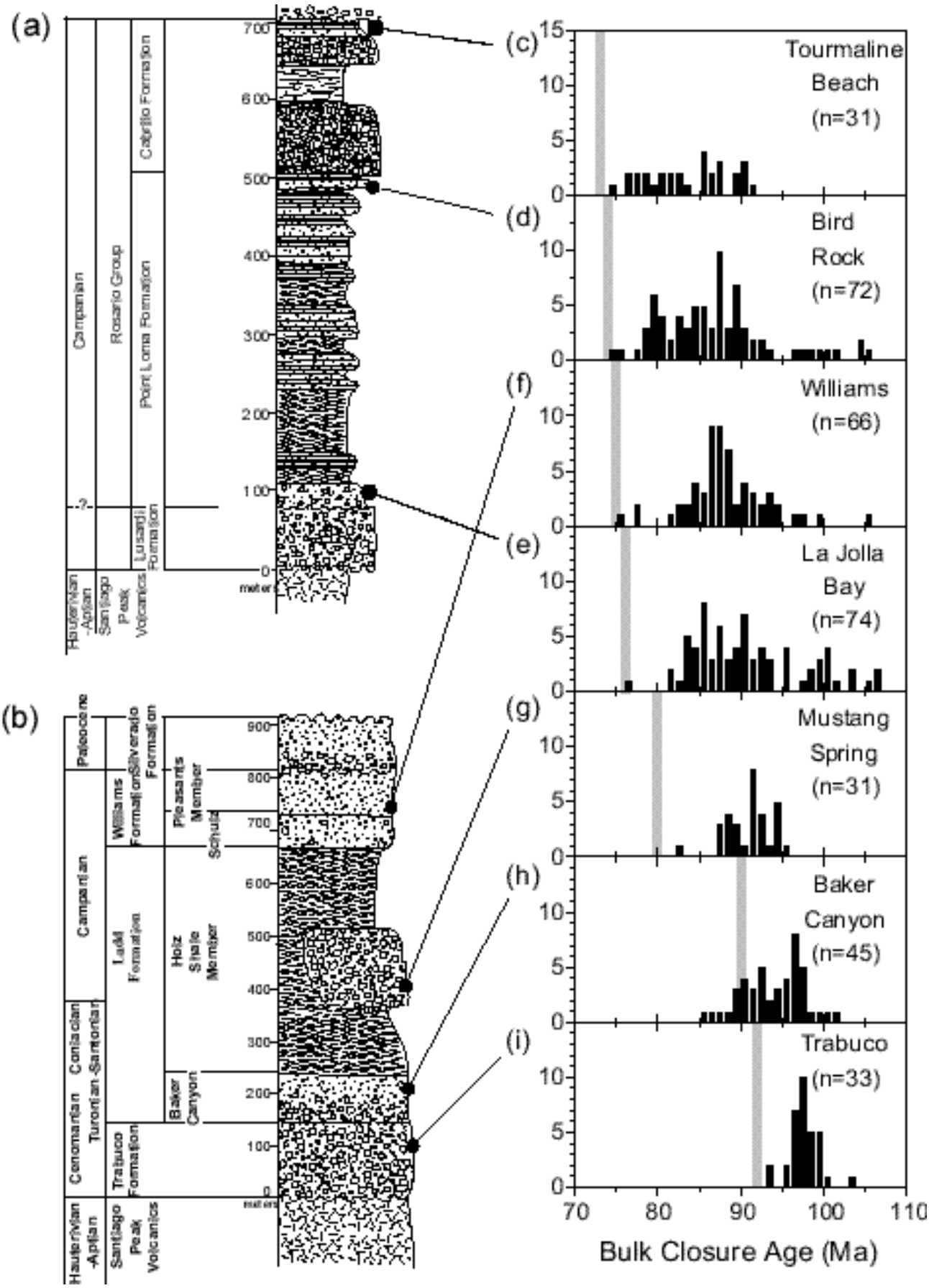

Figure 4: Stratigraphy of PRB forearc strata in (a) San Diego area and (b) northern Santa Ana Mountains. (c)-(i) Histograms of measured detrital K-feldspar closure age distributions

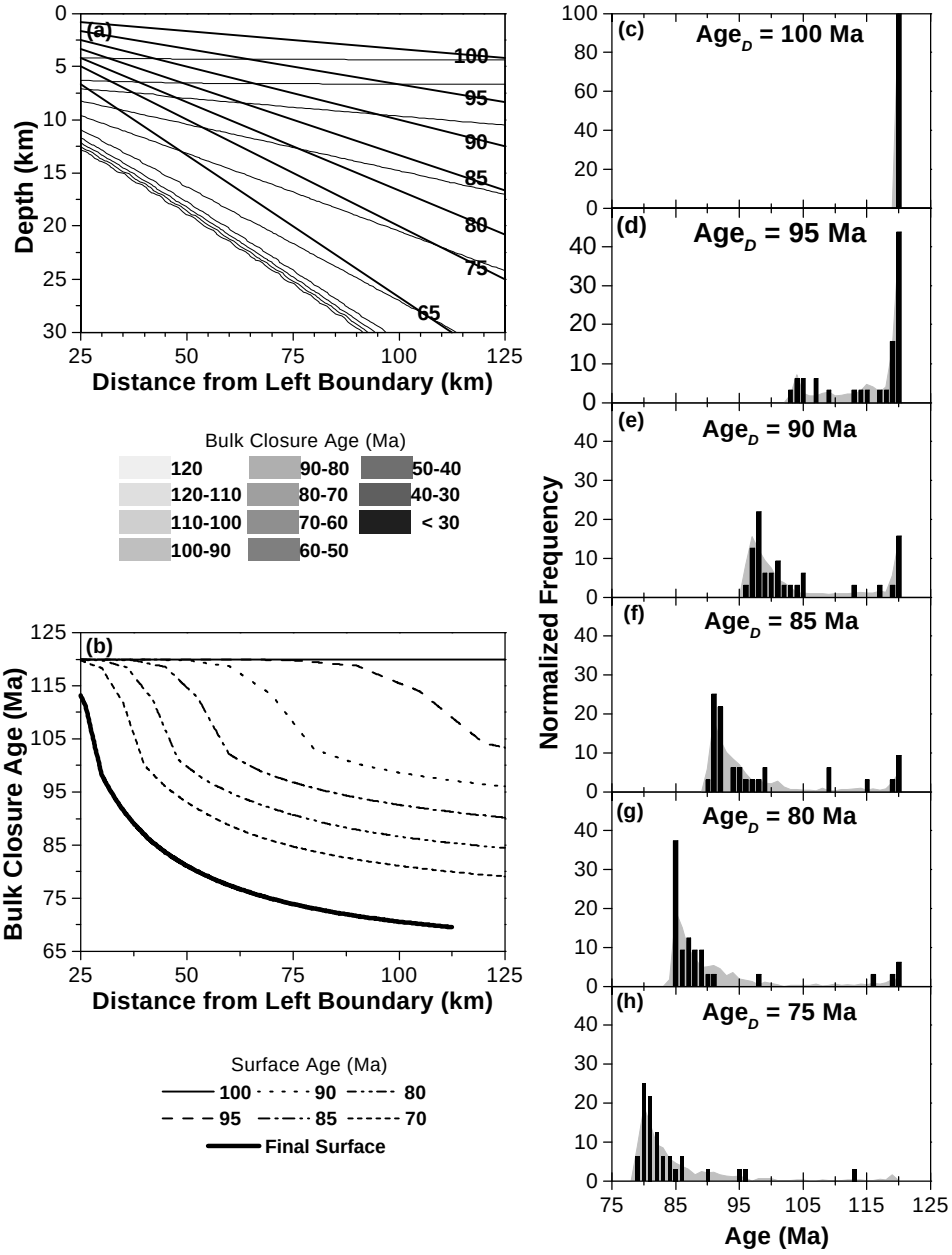

Figure 5: Model I results: (a) Contour plot of final K-feldspar bulk closure age distribution (10 Ma contour interval). Surface positions every 5 m.y. after initial denudation are represented by labeled black lines. The final (65 Ma) surface is a bold line; (b) basement surface mineral age profiles at indicated times; (c)-(h) Histograms of detrital K-feldspar closure ages at indicated times. For each stratigraphic horizon, we overlay distributions calculated from 32 (black) and 1000 (shaded) random samples. All data normalized to 100.

throughout the grid (Figure 5a) reflects the interplay between temperature changes produced by denudation, accumulation of radiogenic ^{40}Ar ($^{40}Ar^*$), and $^{40}Ar^*$ loss by diffusion. In the absence of denudation, protolith ages (= 120 Ma) occur at 0-4 km depths while closure ages between 120-105 Ma are horizontally distributed between 4-7 km (Figure 5a). The onset of denudation at 105 Ma allows samples initially deeper than ~7 km to begin to retain Ar as they approach the surface. The more rapid the denudation, the less time is required for a sample at a given depth to close with respect to $^{40}Ar^*$ loss. After denudation ceases at 65 Ma, isotherms rapidly achieve a steady-state configuration (Figure 5a).

Closure age distributions (Figure 5c-h) relate directly to corresponding surface age profiles (Figure 5b). Note that the 100 Ma surface formed 5 m.y. after the onset of tilting in Model I exposes only rocks from the upper <5 km (< 200°C) of the crust. Because K-feldspars from these depths have retained much all of their $^{40}Ar^*$, protolith ages are largely

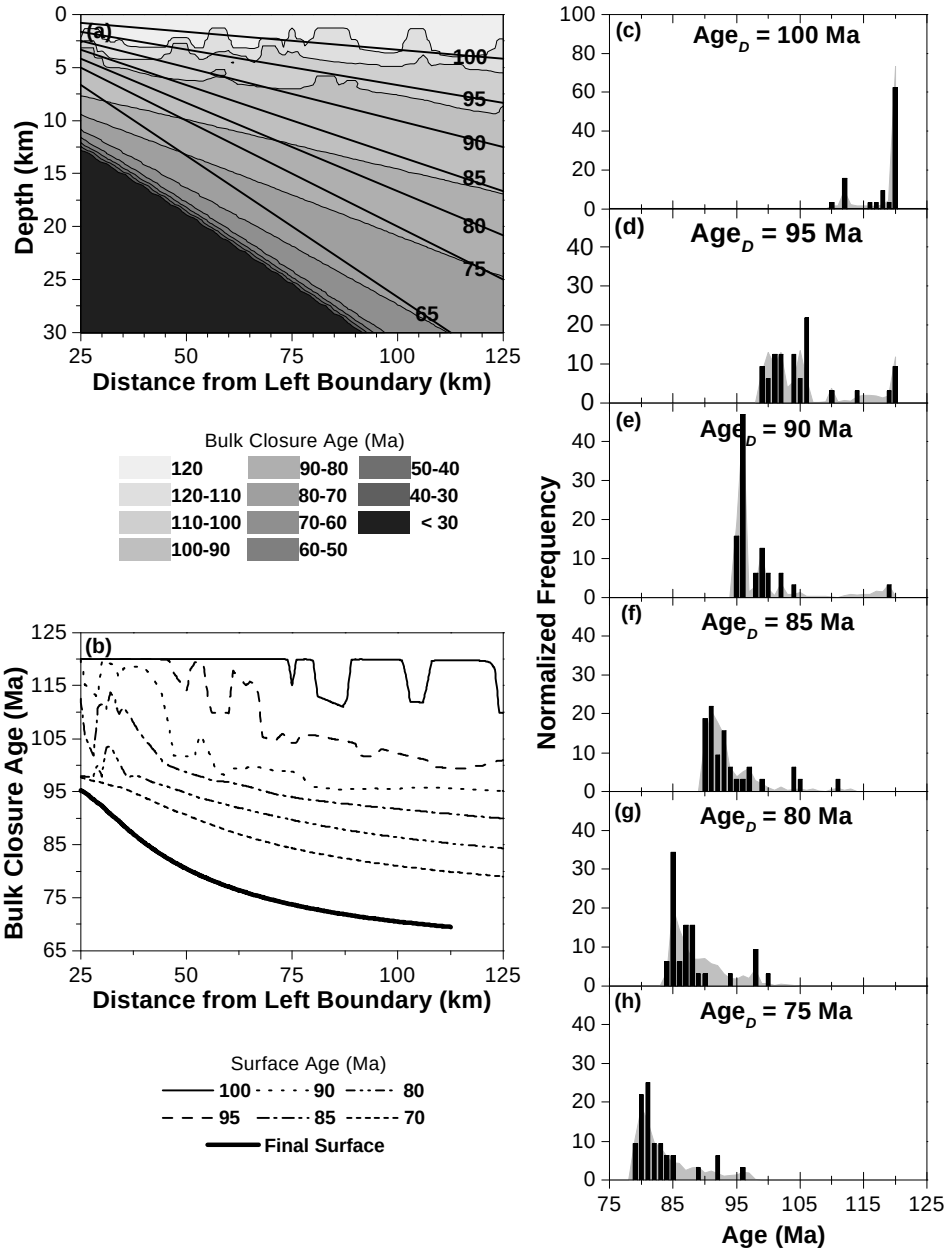

Figure 6. Model II results. See Figure 5 for an explanation of (a)-(h).

preserved. By 95 Ma, continued denudation has begun to expose partially outgassed K-feldspars (i.e. those originating from below 4 km; Figure 5a). By 90 Ma, most K-feldspars exposed at the surface were open to Ar loss prior to 105 Ma (Figure 5b). Despite this, shallow levels sampled from the left portion of the grid continue to yield protolith ages. This results in bimodal closure age distributions (Figure 5c-h). The skewed character of the younger age maxima is a direct consequence of the proportionality between the amount of material eroded and the denudation rate which increases from left to right across the grid. With continued denudation the percentage of results contributing to the younger age maxima grows at the expense of samples recording protolith ages. At the same time the lag between Age_D and the lower age maxima systematically decreases until ~80 Ma (i.e., 25 m.y. after the onset of denudation). Note that exhumation rates calculated from the lag time progressively increase in spite of the fact that the mean denudation rate in the model remains constant [see *Garver and Brandon*, 1994a]. This discrepancy is a manifestation of the sluggish rate at which steady state temperature distributions are approached at this denudation rate.

4.2.2. Overlapping Intrusion and Denudation. The uniformly varying age trends observed in Model I are disrupted when intrusion overlaps denudation (Model II, Figure 6). A prominent effect of magmatic heating upon K-

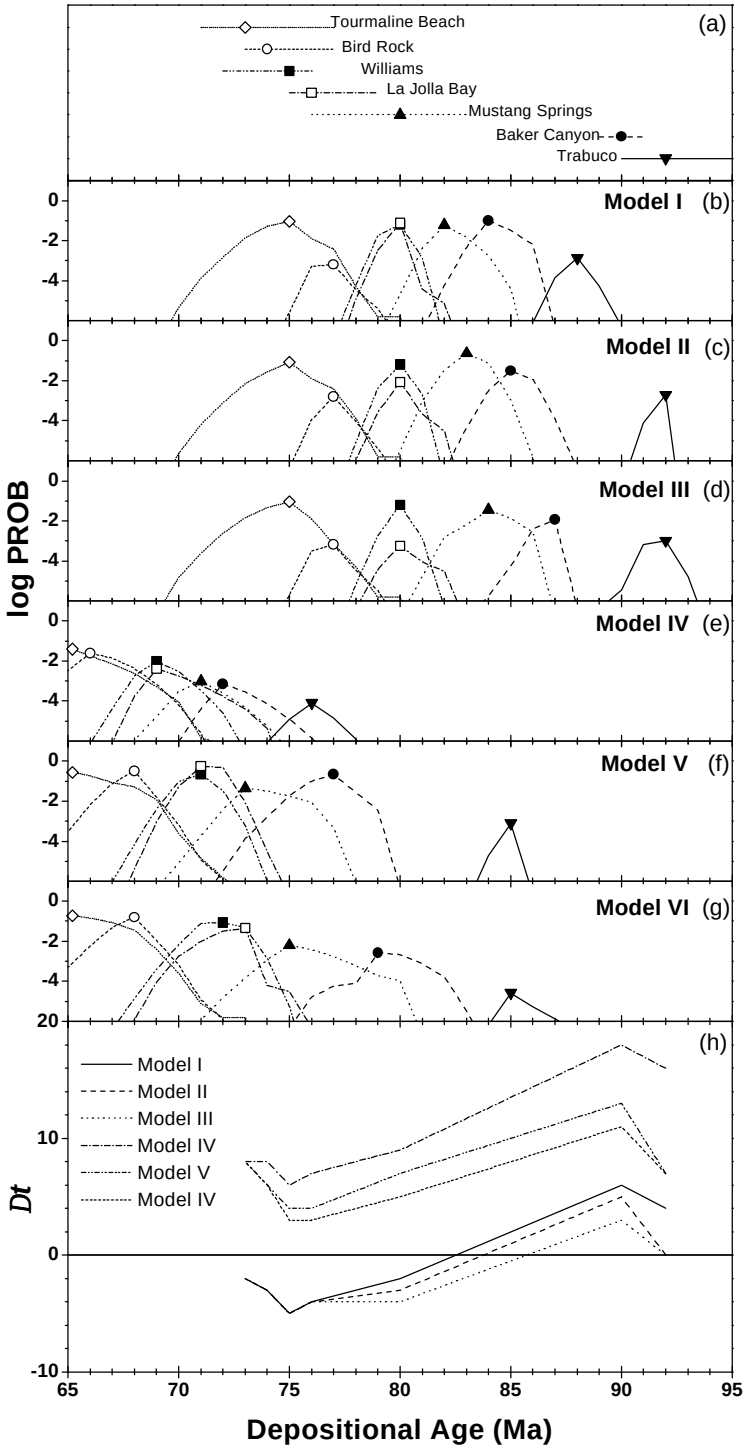

Figure 7. (a) Depositional ages and uncertainties for each samples (see Table 1). (b) -(g) Model I-VI results (see Figure 2 caption). $PROB_{max}$ values represented by symbols defined in Figure 7a (see Table 3). (h). Depositional age versus *Dt* models based upon Figures 7b-7g.

feldspar is that significantly fewer grid positions preserve protolith ages, particularly below 2 km depth (compare Figures 5a and 6a). The distribution of apparent ages at shallow positions within the grid directly reflects the sequence of intrusion at depths ≤ 7 km (compare Plate 2a and Figure 6a). In contrast, the distribution of closure ages at greater depths is insensitive to intrusion and closely resembles Figure 5a. The latter is true because tilting outlasts intrusion by 30 m.y. Features of surface age profiles that are clearly related to individual plutons (Figure 6b) persist at 95 Ma but are

Table 2 Denudation Models

Model	Timing Ma	Mean Denudation Rate[a] Km m.y.$^{-1}$	Mean Cumulative Denudation[b] km	Cumulative Rotation deg
D1	105-65	0.50	20	14.9
D2	105-65	0.25	10	7.6
D3	105-92	0.50	6.5	5.0
	92-89	1.25	10.3	7.8
	89-78	0.15	11.2	8.9
	78-65	0.45	17.8	13.5

[a1]Mean rate corresponds to a horizontal position of 75 km
[b]Mean denudation corresponds to a horizontal position of 75 km.

largely obliterated by 90 Ma (i.e., 5 m.y. after final intrusion). Although Model II closure age distributions differ from model I for older sediments, the results converge at later times (compare Figures 5f-h with Figures 6f-h).

4.2.3. Systematic Analysis of Intrusion and Denudation Effects. Inspection of Figure 7 and Table 3 clearly indicates that for the case in which exhumation outlasts intrusion, denudation rate is the dominant control in determining bulk closure age distributions from K-feldspar. All models characterized by a mean denudation rate of 0.5 km m.y.$^{-1}$ (Models I, II, and III) predict similar depositional ages for each of the samples examined (compare Age_D^{max} values in Figures 7b, 7c, and 7d). For these runs, only the oldest sample (Trabuco = 92 Ma.) is markedly sensitive to the intrusion history (Figure 7h). Values of *Dt* produced by each of the models are generally ± 5 m.y. with all runs yielding identical results by 76 Ma. (Figure 7i). In contrast, reducing the denudation rate by a factor of two produces discernable differences in closure age distributions for contrasting sequences of intrusion. Moreover, all predicted ages are shifted 10-20 m.y. to younger values (Figure 7e-g).

4.2.4. Varying the Time of Initial Denudation. Once a significant proportion of the grid has been denuded by >7 km the detrital closure age systematics depend primarily upon the magnitude of the denudation rate. Consequently, beginning denudation earlier than 105 Ma has little impact upon the results. For example, when denudation begins at 115 Ma, *Dt* values for Trabuco and Baker Canyon decrease by only 1 m.y. (relative to Model I) while those of the younger samples remain unaffected. This is expected since the mean denudation is occurring between 105 and 92 Ma is 6.5 km. In contrast, starting denudation 5 m.y. later (at 100 Ma) has a somewhat greater effect because an insufficient amount of denudation (mean value of 4 km) occurs prior to Trabuco deposition. As a result *Dt* values for the Trabuco and Baker Canyon samples increase by 3 and 2 m.y. respectively while those of the younger samples increase by 1. Although slower denudation is more sensitive to the time of initial denudation, this is counteracted by pervasive intrusion. In summary, while our approach is highly sensitive to the exhumation rate, it is only able to place lower bounds on the amount of denudation that has taken place.

4.2.5. Varying the Diffusion Parameters. Our use of a single domain diffusion model to calculate bulk closure ages may at first glance seem problematic when applied to K-feldspar. Degassing experiments performed with K-feldspar, including those performed at the scale of single crystals [e.g., *Richter et al., 1991*], reveal non-linear Arrhenius behavior consistent with the existence of discrete diffusion domains that vary in length scale and volumetric fraction [e.g., the multi-diffusion domain or MDD model, *Lovera et al.,* 1989]. What is important in our statistical appraisal of the distribution of bulk closure ages in detrital samples, however,

Table 3 Summary of Model Results

Run	Intrusive History[1]	Denudation History[2]	Tourmaline Beach		Bird Rock		La Jolla Bay		Williams		Mustang Springs		Baker Canyon		Trabuco	
			Dt (Ma)	log_m	*Dt* (Ma)	log_m	*Dt* (Ma)	log_m	*Dt* (Ma)	log_m	*Dt* (Ma)	log_m	*Dt* (Ma)	log_m	*Dt* (Ma)	log_m
I	*n/a*	*D1*	-2	-1.0	-3	-3.2	-4	-1.1	-5	-1.2	-2	-1.2	+6	-1.0	+4	-2.9
II	*I1*	*D1*	-2	-1.1	-3	-2.8	-4	-2.0	-5	-1.1	-3	-0.5	+5	-1.5	0	-2.7
III	*I2*	*D1*	-2	-1.1	-3	-3.2	-4	-3.2	-5	-1.2	-4	-1.4	+3	-1.9	0	-2.9
IV	*n/a*	*D2*	+8	-1.5	+8	-1.6	+7	-2.4	+6	-2.0	+9	-2.9	+18	-3.1	16	-4.2
V	*I1*	*D2*	+8	-0.6	+6	-0.5	+4	-0.2	+4	-0.6	+7	-1.3	+13	-0.6	7	-3.1
VI	*I2*	*D2*	+8	-0.8	+6	-0.8	+3	-1.3	+3	-1.1	+5	-2.1	+11	-2.6	7	-4.6
VII	*n/a*	*D3*	+1	-0.4	+1	-0.1	0	-1.5	+1	-0.9	+2	-1.0	+5	-1.1	+2	-3.8
VIII	*I1*	*D3*	+1	-0.3	+1	-0.4	0	-2.7	+2	-0.7	+2	-1.8	+1	-1.6	0	-2.7
IX	*I2*	*D3*	+1	-0.4	+1	-0.2	0	-2.6	+1	-0.8	0	-1.8	0	-1.8	0	-2.3

[1]See Plate 2
[2]See Table 2
$\Delta t^i = Age_S^i - Age_D^{max,i}$ (see text for details).
$log_m = log(PROB_{max})$

is the extent to which MDD behavior is randomly manifested in different K-feldspar grains rather than the complexity of the diffusion behavior itself. Of the diffusion parameters, E and, to a lesser extent log D_o/r_o^2, are most important for relating bulk age to thermal history. A survey of the diffusion properties of a diverse array of basement K-feldspars including representatives from the PRB [*Lovera et al*., 1997] indicates that E and log D_o/r_o^2, are highly correlated. Besides, they define normal distributions characterized by 46 ± 6 kcal mol^{-1} and 5 ± 1 s^{-1} respectively [see *Lovera et al.*, 1997, Figure 3]. To determine how this property affects our results, we reran Model I after randomly assigning E and log D_o/r_o^2 values from the Gaussian distributions to individual grid points [see *Lovera et al.*, 1997, Figure 8]. Taking random variation of diffusion parameters into account causes calculated ages to vary by up to ±4 Ma respect the original calculation but does not significantly affect the characteristics of the closure age distributions. For example, Dt and log($PROB_{max}$) values obtained from model results employing variable diffusion parameters in Table 3 are essentially unchanged from the case in which E and log D_o/r_o^2 were held constant. Hence it appears that to the extent variability in K-feldspar diffusion properties are randomly manifested, the use of the constant K-feldspar diffusion parameters will not prejudice our interpretation.

5. Discussion

The model just presented provides a statistical framework for quantitatively evaluating batholith exhumation histories from derivative sedimentary debris. Use of detrital age distributions to constrain basement exhumation rates depends upon the fidelity of the sedimentary record in documenting the complete spectrum of closure ages that characterize the erosion surface at a given time. The degree to which such a sampling is provided by forearc strata is uncertain and likely depends a great deal upon the tectonic setting [*Dickinson*, 1995]. Consequently, examination of multiple localities throughout the forearc region is probably required to draw firm conclusions regarding batholith exhumation histories. The effort required for obtaining statistically meaningful sampling dictates that focus be placed upon a single mineral thermochronometer. Below we consider the pros and cons of using K-feldspar as a detrital thermochronometer. We then demonstrate how basement exhumation rates may be deduced by fitting the detrital K-feldspar results from the PRB forearc.

5.1 Advantages and Potential Pitfalls of K-feldspar as a Detrital Thermochronometer

K-feldspar offers distinct advantages over other minerals as a detrital thermochronometer. Its moderate Ar retentivity [*Lovera et al.*, 1997] endows it as an ideal monitor of processes active in the mid- to upper crust and allows it to preserve basement thermal history information during modest [< 4 km; Mahon et al., 1998] burial in sedimentary basins. Apatite by comparison is highly susceptible to resetting by burial metamorphism. While Ar diffusion in K-feldspar takes place at temperatures that overlap those required to anneal fission tracks in zircon, the nominal precision of individual detrital K-feldspar dates (± 0.5%) is an order of magnitude better than for zircon. Finally, single crystal total-fusion $^{40}Ar/^{39}Ar$ age analysis can be fully automated so that large, statistically meaningful data sets can be obtained with relative ease compared to fission track methods. Below we consider potential difficulties that might hinder use of K-feldspar as a detrital thermochronometer.

5.1.1. Diagenetic Alteration. In thermochronologic analysis of detrital minerals, we are required to interpret their ages purely in terms of diffusive loss that occurred during basement residence. This interpretation is valid to the extent that $^{40}Ar^*$ distributions are not modified by diagenetic processes and/or high burial temperatures. The relative shallow burial depth experienced by the oldest samples we have examined [<2 km for Trabuco and Baker Canyon samples; *Schoellhamer et al*., 1981] allow us to confidently rule out post-deposition diffusive Ar loss [see *Mahon et al*., 1998]. Despite this, K-feldspar is not immune from diagenetic alteration [*Lee and Parsons*, 1998]. Moreover, authigenic overgrowths on detrital grains are potentially problematic for age analysis [*Girard and Onstott*, 1991; *Aleinikoff et al.*, 1993]. Anomalous young closure ages such as those yielded by the Baker Canyon sample (Figure 4h) may be due to either or both of these phenomena. Uptake of unsupported $^{40}Ar^*$ is yet another potential difficulty. The generally negligible concentrations of excess $^{40}Ar^*$ revealed in step-heating experiments performed with K-feldspars derived from PRB basement exposures [*Grove*, 1993] give us no reason to suspect that excess $^{40}Ar^*$ is a significant problem affecting our detrital K-feldspars age distributions.

Sampling Bias Because tonalite, quartz diorite, and gabbroic lithologies constitute much of the PRB [e.g., *Silver and Chappell*, 1988; *Todd et al*., 1988], our detrital K-feldspar sample certainly fail to uniformly represent all lithologies. Fortunately, volumetrically minor granitic pegmatite and granodiorite is sufficiently widespread throughout the PRB [*Todd et al*., 1988] that regional sampling bias seems unlikely. While it is clear that a phase that is modally important in most lithologies present would provide superior sampling, obvious candidate such as biotite, may present other difficulties such as higher susceptibility to alteration [e.g., *Mitchell and Taka*, 1984].

5.2. More Realistic Thermo-kinetic Models for Batholith Evolution

While our model adequately simulates effects for regional tilting and random intrusion, it requires modification to describe realistic tectonic environments within magmatic arcs where the interplay between faulting, erosion, topographic development, and sedimentation may be complex [*Einsele*, 1992; *Busby et al.*, 1998]. Incorporation of these effects into the model could significantly affect the denudation histories we obtain. Similarly, more realistic treatment of the dynamics of magma intrusion and concomitant wall rock deformation could also cause us to alter our conclusions. Fortunately, faulting and topographic effects can be easily modeled by modifying how the position of the erosion surface within the grid is defined as a function of time.

Refinement of Constant Denudation Models

Refinement of the constant denudation models results displayed in Fig.7 is easily accomplished. The sign of Dt pertaining to a given depositional age (Figure 7) indicates whether prior denudation should be increased or decreased. Specifically, positive values require faster denudation and

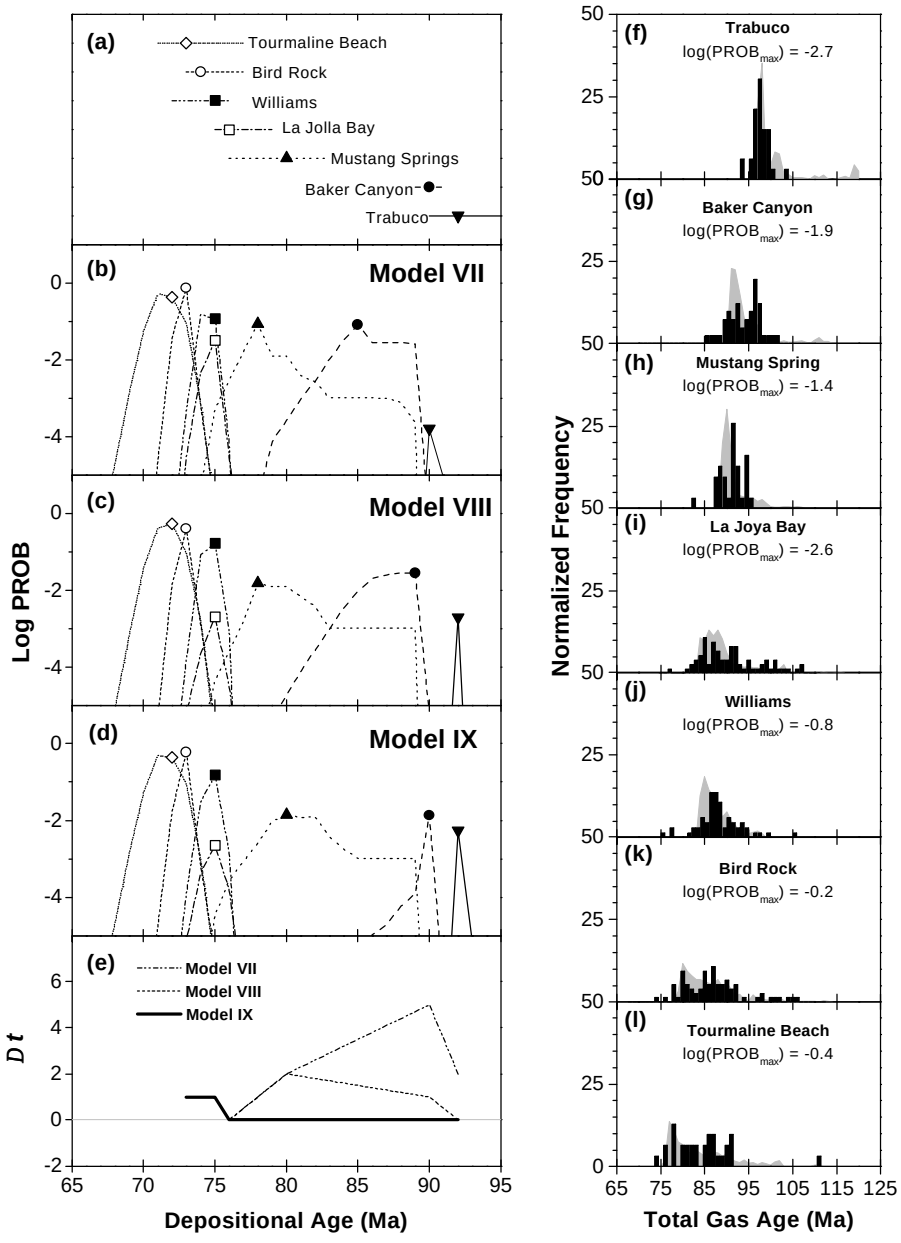

Figure 8: Ability of variable rate denudation models to fit measured closure age distributions. (a) Depositional ages and uncertainties for measured samples. (b)-(d) Model VII-IX results (see Figure 7 caption for explanation; Table 3). (e) Deviation of Age_D^{max} from estimated stratigraphic ages in models VII-IX. (f)-(l) Comparison of measured detrital closure age with those of model IX. All data are normalized to 100.

vice versa. Because the initial denudation rate affects the value required at later times, we first match results from the oldest sample and then proceed to younger strata. Of the initial six simulations, model III produces the best agreement with the measured closure age distributions (Figure 7h). Fortuitous agreement between the model III results and measured values for the oldest sample ($Dt_{Trabuco} = 0$) led us to begin denudation history *D3* at the same rate as *D1* (0.5 km m.y.$^{-1}$; Table 2) and then increase denudation after deposition of the Trabuco sample to fit the next youngest sample (i.e., Baker Canyon). The magnitude of the adjustment to the denudation rate was determined from model III. Specifically, the net denudation between deposition of the Trabuco and Baker Canyon samples is given by [$Age_{D,\ Trabuco}^{max}$ - $Age_{D,\ BakerCyn.}^{max}$] × *D1* = (92 Ma-87 Ma) × 0.5 km/m.y. or 2.5 km. Thus, increasing the denudation rate by a factor of 2.5 (i.e.,

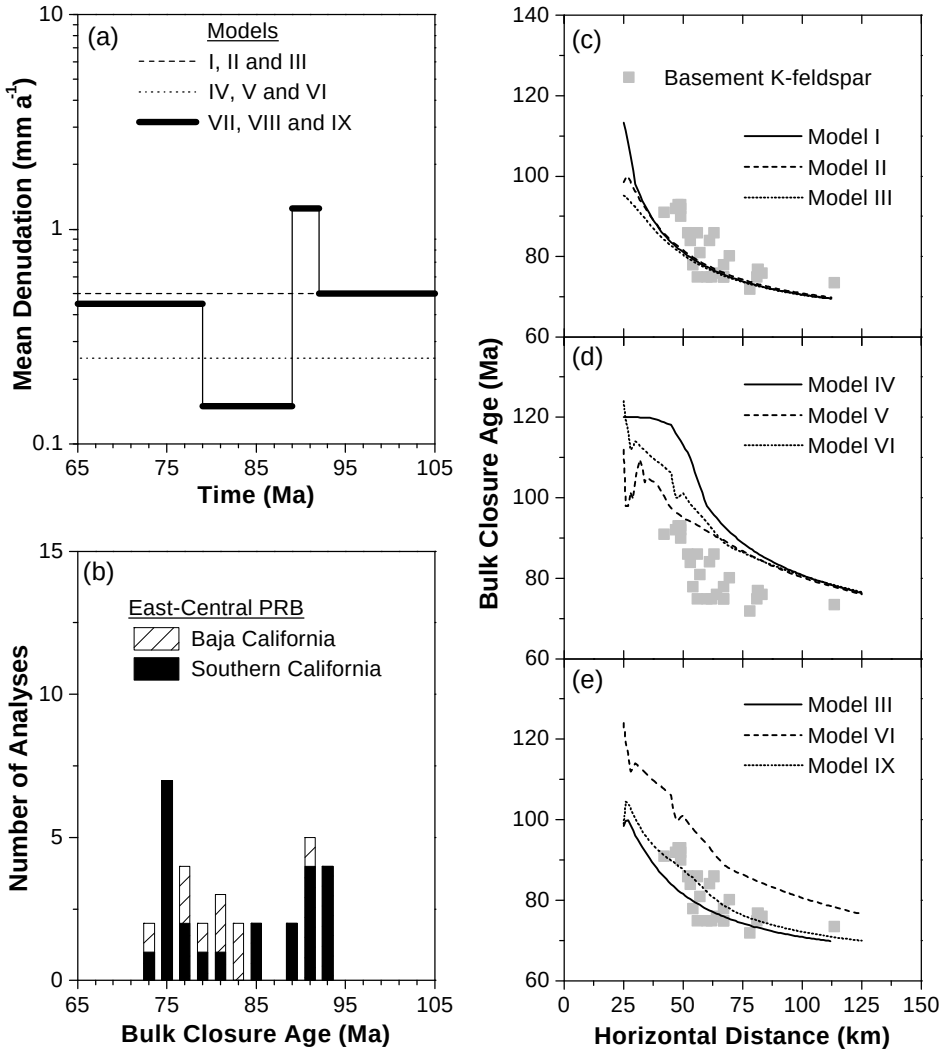

Figure 9: (a) Mean denudation rate vs. time for indicated models (b) Histogram of bulk closure ages (= total fusion ages) calculated from $^{40}Ar/^{39}Ar$ step-heating of K-feldspars from east central PRB [*Grove*, 1993; *Rothstein*, 1997] (see Figure 3 for location). (c)-(e) Comparison of models I-IX results with measured basement K-feldspar ages vs. horizontal distance.

from 0.5 to 1.25 km m.y.$^{-1}$) at 92 Ma reduces *Dt* for Baker Canyon from 3 to zero (Table 3). Equivalent calculations indicate that shortly after 90 Ma, the denudation rate should be decreased to 0.15 km yr^{-1} to reduce *Dt* for the Mustang Spring sample to zero. Likewise increasing the denudation rate at 79 Ma to 0.45 km m.y.$^{-1}$ minimizes *Dt* values for the younger samples to 1 m.y. or less.

Errors in depositional age and/or the time of initial denudation could appreciably affect details of the variable denudation model deduced above. For example, the magnitude of the mean denudation rate between 92-90 Ma (Table 2) is critically dependent upon the depositional ages of the Trabuco and Baker Canyon samples (Table 1). Regardless of this uncertainty, strong overlap of depositional age and measured detrital closure ages for the Baker Canyon sample (Figure 4c-4d) necessarily require higher denudation rates to prevail at ca. 90 Ma than at later times.

Model closure age distributions obtained using the *D3* denudation history are compared with our measured values in Figure 8b-8d. Just as in the case for *D1*, the cumulative denudation produced in *D3* is sufficiently high that only the closure age distributions of the older samples are differentially affected when distinct intrusion histories are imposed (compare Figure 7h with Figure 8e). Note that while *Dt* values for each of the samples are 1 m.y., or less in the case of Model IX, major improvements in $PROB_{max}$ over values obtained in the constant denudation models were not realized. Because the lowest $PROB_{max}$ values are yielded by the oldest samples, it appears likely that in detail, the *I2* intrusion history is inappropriate for the PRB. For example, inspection of the predicted and measured closure age distributions for the Trabuco sample in Figure 8g reveals closure age maxima at ~118 and 103 Ma that reflect significant shallow level intrusion at this time (Plate 2b).

These features alone account for the low $PROB_{max}$ value yielded for this sample. Similarly, the 92 Ma maxima exhibited for the Baker Canyon sample (Figure 8h) might be unduly influenced by pervasive invasion of the eastern batholith at ~10-15 km depths by granitoids of this age (Plate 2b). Younger samples are less affected by intrusion and in general yield higher $PROB_{max}$ values.

5.4. Comparison With Basement Thermochronology From the PRB

The variable denudation model (*D3*) arrived at in section 5.3 (Figure 9a) turns out to be quite consistent with independent basement thermochronology in the northern PRB [*Krummenacher et al*., 1975; *Goodwin and Renne*, 1991; *George and Dokka*, 1994; *Grove*, 1993]. *George and Dokka*, [1994]; and *Grove*, [1993] have revealed the importance of both late batholithic cooling (100-90 Ma) and delayed cooling more than 10 m.y. after final intrusion during the Late Cretaceous (> 80 Ma) [*Krummenacher et al*., 1975; *Goodwin and Renne*, 1991; *Grove*, 1993]. Late batholithic cooling appears to have coincided with a major episode in the tectonic development of the batholith. As summarized in *Busby et al.* [1998] suturing of a fringing island arc to the continental margin coupled with development of a more compressive strain regime appear to have produced a relatively high-standing continental arc by ca. 100 Ma. Of perhaps even greater importance is the likelihood that roughly half the intrusive mass of the PRB appears to have been emplaced between 98 and 92 Ma. In contrast, post 80 Ma. postbatholithic cooling appears to have been triggered by an important shift in tectonic regime from normal subduction to rapid, shallow-inclination subduction [e.g., *Coney and Reynolds*, 1977]. Adjacent Cordilleran magmatic arcs including the Sierra Nevada batholith [e.g., *Dumitru*, 1990] record a cooling signature attributable to shallow inclination subduction.

To illustrate the concordance of the basement and detrital K-feldspar results, K-feldspar total gas ages from the PRB basement [*Grove*, 1993, *Rothstein*, 1997] are plotted in histogram form in Figure 9b and as a function of lateral distance perpendicular to the axis of the batholith in Figures 9c-9e. Episodes of comparatively rapid denudation deduced from the detrital results (Figures 9a) correlate well with age maxima of K-feldspars from PRB basement exposures (Figure 9b). The distribution of K-feldspar total gas ages predicted by the *D1* models agree reasonably well with those measured from the basement regardless of intrusion history (Figure 9c). In contrast, ages predicted by the *D2* models are far older than those observed at a given lateral position (Figure 9d). The best agreement however, is obtained for the D3 models (Figure 9e).

The main difficulty of the *D3* exhumation model for the PRB is the deep level of exposure predicted for the easternmost batholith. While the mean denudation produced by model *D3* (18 km; Table 2) is comparable to available paleodepth estimates for the central and eastern batholith [12-20 km; *Ague and Brimhall*, 1988; *Todd et al*., 1988; *Grove*, 1993; *George*, 1993; *Rothstein*, 1997], lower crustal exposures comparable to those predicted by the model (up to 35 km) do not occur along the eastern margin of the PRB or in the probable eastward continuation of the batholith in mainland Mexico [*Silver and Chappell*, 1988]. Increasing the ambient geothermal gradient and/or shortening the duration of exhumation would readily resolve this discrepancy.

6. Conclusions and Future Research Directions

The similarity of denudation histories deduced from K-feldspar sampled from either the forearc or basement exposures and their sensitivity to long-term exhumation rates (Figure 9) prompt us to conclude that analysis of closure age distributions of detrital minerals in the manner we advocate is quite promising. The major limitation resides in the ability to accurately determine depositional ages. Work in progress is focused upon automating the method to fully explore the range of equivalent solutions that are capable of reproducing the measured data. When extended to additional measurements of closure age distributions elsewhere along the western margin of the PRB we anticipate that it will be possible to refine our approach sufficiently to identify along-strike variations in exhumation history that relate to the nature of the underlying crust and/or other fundamental properties.

Appendix A: $^{40}Ar/^{39}Ar$ Analysis of Detrital K-feldspars

Sandstone samples were crushed, ultrasonically washed in 3% H_2SO_4 solution to remove interstitial calcite cement, and sized to between 35-50 mesh (300 and 500 μm diameter). Detrital feldspars were then concentrated by applying conventional density and magnetic methods. Basement-derived K-feldspars (i.e., grains whose cleavage development and coloration were consistent with orthoclase/microcline) were hand selected from these concentrates using a binocular microscope to avoid volcanic sanidine, chert, and other impurities. This procedure was ineffective for avoiding albite. However, as described below, Ca/K ratios yielded by the $^{40}Ar/^{39}Ar$ measurements allowed us to exclude albite analyses after the fact. Following neutron irradiation in the H-5 position of the Ford Reactor (University of Michigan), grains were fused with a continuous 5 W Ar ion laser and analyzed with a VG3600 rare gas mass spectrometer. Calculated J-factors calculated varied from 0.0054-0.0057 depending upon position and assume an age of 27.8 Ma for Fish Canyon sanidine. Tabulated $^{40}Ar/^{39}Ar$ results and additional experimental details may be obtained from http:\\oro.ess.ucla.edu.

In an attempt to avoid biasing results with data from partially molten grains that were able to retain appreciable Ar, we limited grain size to particles that were readily fused with our Ar ion laser (i.e., grains 500 to 300 μm in diameter) but contained sufficient ^{39}Ar for precise isotopic analysis. Alkali feldspars in this size range that contain 15% K_2O are expected to yield 0.8-4x10^{-14} mol ^{39}Ar for a J-factor of ~0.0055. Accordingly, we excluded all $^{40}Ar/^{39}Ar$ analyses that produced anonymously low ^{39}Ar yields (e.g., < 0.8x10^{-14} mol). Generally feldspar grains that were characterized by poor ^{39}Ar yields also gave Ca/K values (>0.1) that indicated they were albite rather than orthoclase/microcline. All analyses with Ca/K > 0.1 were excluded from our analysis regardless of ^{39}Ar yield.

Appendix B: Depositional Ages

Upper Cretaceous marine sedimentary rocks in the San Diego area are assigned to the Rosario Group and include mudstone and sandstone of the Point Loma Formation overlain by sandstone and conglomerate of the Cabrillo Formation [Figure 4a; *Kennedy and Moore*, 1971; *Nilsen and Abbott*, 1981]. Coccolith flora and foraminifera contained within the Point Loma Formation have been assigned by to the late Campanian/early Maastrichtian [*Bukry*, 1994; *Sliter*, 1968]. *Bannon et al*. [1989] subsequently identified a reverse chron within the Point Loma mudstones as 32R (see the *Harland et al.*, 1982 time scale) and concluded that it represented the base of the Maastrichtian. Continuing development of the magnetic polarity time scale however, has revealed two additional reverse chrons in the middle-late Campanian [*Gradstein et al*., 1994]. Based upon ongoing paleontologic analysis (*W.P. Elder*, personal communication, 1996) it appears probable that it is one of the middle-late Campanian reverse chrons that has been detected in the Point Loma Formation and not 32R. Consequently, both the Point Loma and Cabrillo Formations appear Campanian with depositional ages between 77-72 Ma (Table 1).

The geology of the northern Santa Ana Mountains has been mapped and described by *Schoellhamer et al*. [1981] while depositional environments and fossil assemblages are documented in *Bottjer et al*. [1982]. Excellent exposures of the Late Cretaceous strata occur in the Silverado Canyon area (Figure 4b). There unfossiliferous, terrestrial conglomerates, and sandstone of the Trabuco Formation depositionally overlie the volcanic supracrustal cover of the PRB (Figure 4a). The Trabuco Formation is in turn overlain by fossiliferous, marine fan-delta conglomerates and sandstones of Turonian age [*Popenoe*, 1942] that constitute the Baker Canyon Member of the Ladd Formation. The Ladd Formation fines upward into the deep marine, latest Turonian to Campanian Holz Shale Member. Conglomerate-dominated, submarine canyon fill was deposited within the Holz Shale as the Mustang Spring lens (Figure 4b) in the Campanian [*Almgren*, 1982]. Shelf sandstone of the Williams Formation was deposited in late Campanian time (Figure 4b). On the basis of the *Gradstein et al*. (1994) timescale, combined magnetostratigraphy [*Fry et al*., 1985] and faunal constraints (Table 1) indicate that Late Cretaceous sedimentation in the Silverado Canyon area occurred between ~95 to 72 Ma.

Acknowledgments. This work was funded by grants from the DoE and NSF. T.M. Harrison, K.V. Hodges, R.V. Ingersoll, H. Lang, C.E. Manning, R. Rudnick, P. Rummelhart, and an anonymous reviewer are acknowledged for helpful critiques of the manuscript. D.R. Rothstein made available unpublished basement K-feldspar and biotite results from Baja California.

References

Abbott, P.L. and T.E. Smith, Sonora, Mexico source for the Eocene Poway Conglomerate of southern California, *Geology*, 17, 329-332, 1989.

Abdel-Monejm, A.A., and J.L. Kulp, Paleogeography and the source of sediments of the Triassic basin, New Jersey, by K-Ar dating, *Geol. Soc. Am. Bull*., 79, 1231-1242., 1968.

Ague, J.J. and G.H. Brimhall, Regional variations in bulk chemistry, mineralogy, and the compositions of mafic and accessory minerals in the batholiths of California, *Geol. Soc. Am. Bull*., 100, 891-911, 1988.

Aleinikoff J.N., M. Walter, M.J. Kunk, P.P. Hearn, Do ages of authigenic K-feldspar date the formation of Mississippi Valley type Pb-Zn deposits, central and southeastern-United-States: Pb isotopic evidence, *Geology*, 21, 73-76, 1993.

Almgren, A.A., Foraminiferal paleoenvironmental interpretation of the Late Cretaceous Holz Shale, Santa Ana Mountains, in *Late Cretaceous Depositional Environments and Paleogeography, Santa Ana Mountains, Southern California*, edited by D.J. Bottjer, I.P. Colburn, and J.D. Cooper, pp 45-57, Pac. Sect. Soc. Econ. Paleontol.. Mineral., Los Angeles, CA, 1982.

Bannon, J.L., D.J. Bottjer, S.P. Lund and L.R. Saul, Campanian/Maastrichtian stage boundary in southern California: Resolution and implications for large-scale depositional patterns, *Geology*, 17, 80-83, 1989.

Barton, M.D. D.A. Battles, G.E. Bebout, R.C. Capo, J.N. Christensen, S.R. Davis, R.B. Hanson, C.J. Michelsen, and H.E. Trim, Mesozoic Contact Metamorphism in the Western United States, in *Rubey colloquium on Metamorphism and crustal evolution of the Western United States*, Volume VII, pp. 110-178, edited by W.G. Ernst, Prentice Hall, Englewood Cliffs, N. J., 1988.

Bottjer, D.J., I.P. Colburn, and J.D. Cooper, *Late Cretaceous Depositional Environments and Paleogeography, Santa Ana Mountains, Southern California*, Pac. Sect., pp. 121, Soc. Econ. Paleontol. Mineral., Los Angeles, CA, 1982.

Bukry, D., Coccolith correlation of late Cretaceous Point Loma Formation at La Jolla and Carlsbad, San Diego County, California: *U.S. Geol. Sur. Open-File Rep.* 94-678, 23, 1994.

Busby C., D. Smith, W. Morris, and B. Fackler-Adams, Evolutionary model for convergent margins facing large ocean basins: Mesozoic Baja California, Mexico, *Geology*, 26, 227-230, 1998.

Butler, R.H., W.R. Dickinson, and G.E. Gerhels, Paleomagnetism of coastal California and Baja California: Alternatives to large-scale northward transport, *Tectonics*, 10, 561-576, 1991.

Clift, P.D., A. Carter, A.J. Hurford, Constraints on the evolution of the East Greenland Margin: Evidence from detrital apatite in offshore sediments, *Geology* ,24: 1013-1016, 1996.

Coney, P.J., and S.J. Reynolds, Cordilleran Beniof Zones, *Nature*, 270, 403-406, 1977.

Copeland, P., and T.M. Harrison, Episodic rapid uplift in the Himalaya revealed by $^{40}Ar/^{39}Ar$ analysis of detrital K-feldspar and muscovite, Bengal fan. *Geology*, 18, 354-357, 1990.

Corrigan, J.D., and K.D. Crowley, Unroofing of the Himalayas: A view from apatite fission-track analysis of Bengal Fan sediments, *Geophys. Res. Lett.*, 19, 2345-2348, 1992.

Dallmeyer, R.D.; J.D. Keppie and R.D. Nance, $^{40}Ar/^{39}Ar$ Ages of detrital muscovite within Lower Cambrian and Carboniferousclastic sequences in northern Nova Scotia and southern New-Brunswick - Implications for provenance regions, *Can. Jour. Ear. Sci*., 34, 156-168, 1997.

Dickinson, W.R. and R.F. Butler, Coastal and Baja California paleomagnetism reconsidered, *Geol. Soc. Am. Bull.*, 110, 1268-1280, 1998.

Dickinson, W.R., Forearc basins, *in Tectonics of Sedimentary Basins*, edited by R.V. Ingersoll and C.J. Busby, pp. 221-262, Blackwell Sci., Cambridge, Mass., 1995.

Dodson, M. H., Closure temperature in cooling geochronologic and petrologic systems, *Contrib. Mineral. Petrol*., 40, 259-274, 1973.

Dokka, R.K, Fission-track geochronologic evidence for Late Cretaceous mylonitization and Early Paleocene uplift of the northeastern Peninsular Ranges, California, *Geophys. Res. Lett.*, 11, 46-49, 1984.

Dumitru, T.A., Subnormal Cenozoic geothermal gradients in the extinct Sierra Nevada magmatic arc: Consequences of the Laramide and Post-Laramide shallow-angle subduction, *J. Geophys. Res.* 95, 4925-4941, 1990.

Einsele, G., *Sedimentary Basins: Evolution, Facies, and Sediment Budget*, 628pp, Springer-Verlag, 1992.

Engel, A.E.J., and P.A. Schultejann, Late Mesozoic and Cenozoic tectonic history of south central California, *Tectonics*, 3, 659-675, 1984.

Erskine, B.G., and H.R. Wenk, Evidence for Late Cretaceous crustal thinning in the Santa Rosa mylonite zone, southern California, *Geology*, 18, 1173-1177, 1985.

Froude, D.O., T.R. Ireland, P.D. Kinney, I.S. Williams and W.

Compston, Ion microprobe identification of 4,100-4,200 Myr-old terrestrial zircons, *Nature*, 304, 616-618, 1983.

Fry, J.G., D.J. Bottjer, and S.P Lund, Magnetostratigraphy of displaced Upper Cretaceous strata in southern California, *Geology*, 13, 648-651, 1985.

Garver, J.I. and M.T. Brandon, Erosional denudation of the British Clombia Coast Ranges as determined from fission-track ages of detrital zircon from the Tofino basin, Olympic Peninsula, Washington, *Geol. Soc. Am. Bull*., 106, 1398-1412, 1994a.

Garver, J.I. and M.T. Brandon, Fission-track ages of detrital zircons from Cretaceous strata, southern British Columbia: Implications for the Baja BC hypothesis, *Tectonics*, 13, 401-420, 1994b.

Gastil, R. G., M. Wracher, G. Strand, L.L. Kear, D. Eley, D. Chapman, The tectonic history of the southwestern United States and Sonora, Mexico during the past 100 m.y., *Tectonics*, 11, 990-997, 1992.

Gaudette, H.E., A. Vitrac-Michard and C.J. Allegre, North American Precambrian history recorded in a single sample: high-resolution U-Pb systematics of the Potsdam sandstone detrital zircons, New York state, *Earth Planet. Sci. Lett*., 54, 248-260, 1981.

Gehrels, G.E., W.R. Dickinson, G.M. Ross, J.H. Stewart and D.G. Howell, Detrital zircon reference for Cambrian to Triassic miogeoclinal strata of western North America, *Geology*, 23, 831-834, 1995.

George, P.G., Tectonic implications of fission-track thermochronology and amphibole thermobarometry studies of the northern Peninsular Ranges batholith, southern California, Ph. D. thesis, La. State Univ., Baton Rouge, LA, 1993.

George, P.G., and R.K. Dokka, Major Late Cretaceous cooling events in the eastern peninsular ranges, California, and their implications for Cordilleran tectonics, *Geol. Soc. Am. Bull*., 106, 903-914, 1994.

Girard, J.P. and T.C. Onstott, Application of $^{40}Ar/^{39}Ar$ laser-probe and step-heating techniques to the dating of diagenetic K-feldspar overgrowths, *Geochim. Cosmochim. Acta*, 55, 3777-3793, 1991.

Girty, G.H., Sandstone provenances, Point Loma Formation, San Diego, California: Evidence for uplift of the Peninsular Ranges during the Laramide Orogeny, *Jour. Sed. Petrol.*, 57, 839-844, 1986.

Goodwin, L. B., and P. R. Renne, Effects of progressive mylonitization on Ar retention in biotites from the Santa Rosa mylonite zone, California, and thermochronologic implications, *Contr. Mineral. Petrol*., 108, 283-297, 1991.

Gradstein, F.M., F.P. Agterberg, J.G. Ogg, J. Hardenbol, P. Van Veen, J. Therry and Z. Huang, A Mesozoic time scale, *J. Geophys. Res*., 99, 24,051-24,074, 1994.

Grove, M., Thermal Histories of southern California basement terranes, Ph. D. thesis, Univ. of Calif., Los Angeles, 1993.

Hanson R.B., and M.D. Barton, Thermal development of low-pressure metamorphic belts: Results from two-dimensional numerical models, *J. Geophys. Res*. 94, 10363-10377, 1989.

Harland, W.B., Cox, A.V., Llewellyn, P.G., Pickton, C.A.G., Smith, A.G., and Walters, R., *A Geologic Time Scale*, 131 pp., Cambridge Univ. Press, New York 1982.

Harrison T.M., P. Copeland, S.A. Hall, J. Quade, S. Burner, T.P. Ojha and W.S.F. Kidd, Isotopic preservation of Himalayan Tibetan uplift, denudation, and climatic histories of 2 mollase deposits, *Jour. Geol*., 101, 157-175, 1993.

Hurford, A.J., F.J. Fitch and A. Clarke, Resolution of the age structure of the detrital zircon populations of 2 Lower Cretaceous sandstones from the Weald of England by fission-track dating, *Geol. Mag*., 121, 269-277, 1984.

Hutson, F., P. Mann and P. Renne, $^{40}Ar/^{39}Ar$ Dating of single muscovite grains in Jurassic siliciclastic rocks (San-Cayetano Formation) - Constraints on the paleoposition of western Cuba, *Geology*, 26, 83-86, 1998.

Ireland, T.R., T. Flottmann, C.M. Fanning, G.M. Gibson, W.V. Preiss, Development of the early Paleozoic Pacific margin of Gondwana from detrital zircon ages across the Delamerian orogen, *Geology*, 26, 243-246, 1998.

Kelley, S., and B.J. Bluck, Detrital mineral ages from the southern uplands using $^{40}Ar/^{39}Ar$ laser probe, *J. Geol. Soc. London*, 146, 401-403, 1989.

Kennedy, M. P., and G. W. Moore, Stratigraphic relations of Upper Cretaceous and Eocene Formations, San Diego coastal area, California, *Am. Assoc. Pet. Geol. Bull.*, 55, 709-722, 1971.

Kimbrough, D.L., P.L. Abbott, R.G. Gastil and P.J.W. Hamner, Provenance investigations using magnetic susceptibility, *Jour. Sediment. Res*., 67, 879-883, 1997.

Krummenacher, D., R. G. Gastil, J.Bushee, and J. Doupont, K-Ar apparent ages, Peninsular Ranges batholith, southern California: *Geol. Soc. Am. Bull*., 86, 760-768, 1975.

Ledent, D., C. Patterson, and G.R. Tilton, Ages of zircon and feldspar concentrates from North American beach and river sands, *J. Geol*., 72, 112-122, 1964.

Lee, M.R. and I. Parsons, Microtextural controls of diagenetic alteration of detrital alkali feldspars: A case study of the Shap Conglomerate (Lower carboniferous), northwest England, *J. Sed.iment. Petrol*., 68, 198-211, 1998.

Lovera, O.M., F.M. Richter and T.M. Harrison, $^{40}Ar/^{39}Ar$ geothermometry for slowly cooled samples having a distribution of diffusion domain sizes, *J. Geophys. Res*., 94, 17,917-17,935, 1989.

Lovera, O.M., M. Grove, T.M. Harrison and K.I. Mahon, Systematic analysis of K-feldspar $^{40}Ar/^{39}Ar$ step-heating experiments I; Significance of activation energy determinations, *Geochim. Cosmochim. Acta*., 61, 3171-3192, 1997.

Mahon, K.I., T.M. Harrison and M. Grove, The thermal and cementation histories of a sandstone petroleum reservoir, Elk Hills, California. 1; $^{40}Ar/^{39}Ar$ thermal history results, *Chem. Geol*. 152, 227-256, 1998.

McDougall, I. and T.M. Harrison, *Geochronology and Thermochronology by the $^{40}Ar/^{39}Ar$ method*, 240 pp., Oxford University Press, New York, 1999.

Minch, J.A., The late Mesozoic-early Tertiary framework of continental sedimentation, northern Peninsular Ranges, Baja California, Mexico, in *Eocene Depositional Systems, San Diego, California*, edited by P.L. Abbott, pp. 43-68, Pac. Sect., Soc. Econ. *Paleontol. Mineral*., Los Angeles, CA 1979.

Mitchell, J.G., and A.S. Taka, Potassium and argon loss patterns in weathered micas: Implications for detrital mineral studies, with particular reference to the paleogeography of the British Isles, *Sed. Geol.*, 39, 27-52, 1984.

Nilsen, T. H., and P. L. Abbott, Paleogeography and sedimentology of Upper Cretaceous turbidites, San Diego, California, *Am. Assoc. Pet. Geol. Bull*., 65, 1256-1284, 1981.

Ortega Rivera, A., E. Farrar, J.A. Hanes, D.A. Archibald, R.G. Gastil, D.L. Kimbrough, M. Zentilli, M. Lopez Martinez, G. Feraud and G. Ruffet, Chronological constraints on the thermal and tilting history of the Sierra San Pedro Matir pluton, Baja California, Mexico, from U/Pb, $^{40}Ar/^{39}Ar$, and fission-track geochronology, *Geol. Soc. Am. Bull.* 109, 728-745, 1997.

Popenoe, W.P., Upper Cretaceous formations and faunas of southern California, *Am. Assoc.Petrol. Geol. Bull.*, 26, 162-187, 1942.

Press, W.H., B.P. Flannery, S.A. Teukolsky, and W.T. Vetterling, *Numerical Recipes: The Art of Scientific Computing*, 818 pp., Cambridge Univ. Press, New York, 1986.

Renne, P.R., T.A. Becker, and S.M. Swapp, $^{40}Ar/^{39}Ar$ laser probe dating of detrital micas from the Montgomery Creek Formation, Northern California: Clues to provenance, tectonics, and weathering processes, *Geology*, 18, 563-566, 1990.

Richter, F.M., O.M. Lovera, T.M. Harrison, and P. Copeland, Tibetan tectonics from $^{40}Ar/^{39}Ar$ analysis of a single K-feldspar sample, *Earth Planet. Sci. Lett*., 105, 266-278, 1991.

Rothstein, D.A., Metamorphism and denudation of the Eastern Peninsular Ranges batholith, Baja California Norte, Mexico, Ph. D. thesis, Univ. of Calif., Los Angeles, 1997.

Schoellhamer, J.E., J.G. Vedder, R.F. Yerkes and D.M. Kinney, Geology of the Northern Santa Ana Mountains, California, *U.S. Geol. Surv. Prof. Pap.* 420D, 109 p., 1981.

Silver, L. T., and B.W. Chappell, The Peninsular Ranges Batholith: an insight into the evolution of the Cordilleran batholiths of southwestern North America, *Trans. R. Soc. of Edinburgh, Earth Sci.*, 79, 105-121, 1988.

Sliter, W.V., Upper Cretaceous foraminifera from southern California and northwestern Baja California, Mexico: *Kansas Univ. Paleo. Contr*. 49, 141 p, 1968.

Stock J.D. and D.R. Montgomery, Estimating paleorelief from detrital mineral age ranges, *Basin Res*. 8, 317-327, 1996.

Todd, V.R., B.G. Erskine, and D.M. Morton, Metamorphic and tectonic evolution of the northern Peninsular Ranges Batholith,

southern California, *in Metamorphism and Crustal Evolution of the Western United States*, Rubey, Vol. VII:, edited by W. G. Ernst, pp. 894-937, Prentice-Hall, Englewood Cliffs, N. J., 1988.

Walawender, M. W., R.G. Gastil, J.P. Clinkenbeard, W.V. McCormick, B.G. Eastman, R.S. Wernicke, M.S. Wardlaw, S.H. Gunn and B.M. Smith, Origin and evolution of the zoned La Posta-type plutons, eastern Peninsular Ranges batholith, southern and Baja California, in *The Nature and Origin of Cordilleran Magmatism*, edited by J.L. Anderson, *Geol. Soc. Am. Mem*. 174, 1-18, 1990.

P. L. Abbott and D. L. Kimbrough, Department of Geological Sciences, San Diego State University San Diego, CA 92182-1020. (e-mail:)

M. Grove, O. M. Lovera, Department of Earth and Space Sciences, Institute of Geophysical and Planetary Sciences, University of California, Los Angeles, CA 90095-1567. (lovera@ess.ucla.edu.)

(Received May 6, 1998; revised February 18, 1999; accepted March 1, 1999)